HAL
open science

Quantification of carbon fluxes through the tricarboxylic acid cycle in early germinating lettuce embryos

Christophe Salon, Philippe Raymond, Alain Pradet

▶ To cite this version:

HAL Id: hal-02716975

https://hal.inrae.fr/hal-02716975

Submitted on 1 Jun 2020

Quantification of Carbon Fluxes through the Tricarboxylic Acid Cycle in Early Germinating Lettuce Embryos*

Christophe Salon, Philippe Raymond, and Alain Pradet‡

From the Station de Physiologie Végétale, Institut National de la Recherche Agronomique, Centre de Recherche de Bordeaux, BP 131, 33140 Pont de la Maye, France

A method involving labeling to isotopic steady state and modeling of the tricarboxylic acid cycle has been used to identify the respiratory substrates in lettuce embryos during the early steps of germination. We have compared the specific radioactivities of aspartate and glutamate and of glutamate C-1 and C-5 after labeling with different substrates.

Labeling with [U-^{14}C]acetate and $^{14}CO_2$ was used to verify the validity of the model for this study; the relative labeling of aspartate and glutamate was that expected from the normal operation of the tricarboxylic acid cycle. After labeling with $^{14}CO_2$, the label distribution in the glutamate molecule (95% of the label at glutamate C-1) was consistent with an input of carbon via the phosphoenolpyruvate carboxylase reaction, and the relative specific radioactivities of aspartate and glutamate permitted the quantification of the apparent rate of the fumarase reaction.

CO_2 and intermediates related to the tricarboxylic acid cycle were labeled with [U-^{14}C]acetate, [1-^{14}C]hexanoate, or [U-^{14}C]palmitic acid. The ratios of specific radioactivities of asparate to glutamate and of glutamate C-1 to C-5 indicated that the fatty acids were degraded to acetyl units, suggesting the operation of β-oxidation, and that the acety-CoA was incorporated directly into citrate. Short-term labeling with [1-^{14}C]hexanoate showed that citrate and glutamate were labeled earlier than malate and aspartate, showing that this fatty acid was metabolized through the tricarboxylic acid cycle rather than the glyoxylate cycle. This was in agreement with the flux into gluconeogenesis compared to efflux as respiratory CO_2. The fraction of labeled substrate incorporated into carbohydrates was only about 5% of that converted to CO_2; the carbon flux into gluconeogenesis was determined after labeling with $^{14}CO_2$ and [1-^{14}C]hexanoate from the specific radioactivity of aspartate C-1 and the amount of label incorporated into the carbohydrate fraction. It was only 7.4% of the efflux of respiratory CO_2. The labeling of alanine indicates a low activity of either a malic enzyme or the sequence phosphoenol-pyruvate carboxykinase/pyruvate kinase.

After labeling with [U-^{14}C]glucose, the ratios of specific radioactivities indicated that the labeled carbohydrates contributed less than 10% to the flux of acetyl-CoA. The model indicated that the glycolytic flux is partitioned one-third to pyruvate and two-thirds to oxalacetate and is therefore mainly anaplerotic. The possible role of fatty acids as the main source of acetyl-CoA for respiration is discussed.

The germination of seeds begins with water uptake and is completed by the emergence of the radicle. Most studies of reserve metabolism in seeds have been made after germination (*i.e.* after radicle emergence), when the major reserves are being mobilized (Bewley and Black, 1985). Much less is known about the metabolism of germinating seeds. Membranes or enzymes are often considered to be damaged either during drying (Crowe *et al.*, 1987) or during the rehydration which starts the germination process. It is generally assumed that mitochondria are metabolically deficient and that catabolism is restricted to the consumption of readily available substrates such as soluble carbohydrates (Bewley and Black, 1985). It has been established by an *in vivo* study that respiration is the main pathway of ATP regeneration in freshly imbibed lettuce seeds (Hourmant and Pradet, 1981). The substrate used as well as the pathways potentially involved in this process are not known. Lettuce seeds are rich in lipids and proteins but also contain soluble carbohydrates (Mayer and Poljakoff-Mayber, 1963). The degradation of labeled glucose and acetate by germinating lettuce embryos gave a preliminary indication that the tricarboxylic acid cycle might be functional (Raymond *et al.*, 1985a). The respiratory quotient ($CO_2/O_2 = 0.7$) suggests that lipids could be a major respiratory substrate. The aim of this study was to determine the relative contribution of carbohydrates and fatty acids to the carbon supply to respiration. Germinating lettuce embryos have been labeled to steady state with ^{14}C-fatty acids and [^{14}C]glucose, and the distribution of radioactivity in amino acids and organic acids related to the tricarboxylic acid cycle has been studied following the principles developed by Katz and Grunnet (1979). The results indicate that fatty acids are degraded by β-oxidation and suggest that this pathway contributes to at least 90% of the CoASAc flux through the tricarboxylic acid cycle, whereas the role of glycolysis appears to be mainly anaplerotic.

EXPERIMENTAL PROCEDURES

Materials

Lettuce seeds (*Lactuca sativa*, cv. Val d'Orge), supplied by Etablissements Clause (Bretigny sur Orge, France), were decontaminated as previously described (Raymond and Pradet, 1980) and imbibed in sterile water at 20 °C for 2 h. The endosperm, which is impermeable to most substrates, was then removed, and the embryos were used for the labeling experiments. Controls for bacterial or fungal contamination were done for each experiment (Raymond and Pradet, 1980). All enzymes were obtained from Sigma. Labeled substrates were

purchased from Commissariat à l'Energie Atomique (Gif-sur-Yvette, France).

Labeling and Extraction

Embryos were placed in 15-ml vials with 1 ml of sodium phosphate buffer (0.02 M, pH 6.5) containing one of the labeled substrates: D-[U-^{14}C]glucose (11 GBq/mmol, 220 KBq, 20 μM), [U-^{14}C]acetate (3.5 GBq/mmol, 37 KBq, 11 μM), [U-^{14}C]palmitic acid (15 GBq/mmol), 74 KBq, 5 μM), sodium [^{14}C]bicarbonate (2.1 GBq/mmol, 370 KBq, 180 μM), and sodium [1-^{14}C]hexanoate (0.7 GBq/mmol, 150 KBq, 210 μM). The center well contained 0.2 ml of 5% (w/v) KOH on filter paper for CO$_2$ collection. The vials were stoppered and placed on an agitated table at 20 °C for various times. At the end of incubation, the vials were placed on ice; the embryos were rinsed with ice-cold water and extracted; and the anionic, cationic, and neutral fractions were prepared according to Stitt and ap Rees (1978).

The labeling time chosen for isotopic steady-state labeling was 6 h; at the end of incubation, the embryos had been imbibing for 10 h, a time still characteristic of the germination period (Raymond *et al.*, 1985a).

Analytical Methods

Specific Radioactivity of Amino Acids—An aliquot of the amino acid fraction was analyzed by HPLC[1] essentially as described by Burbach *et al.* (1982) after derivatization with o-phthaldialdehyde. 20 μl of extract corresponding to four embryos were mixed with 20 μl of the o-phthaldialdehyde reagent, and 20 μl were injected after exactly 2 min on a reverse-phase column (CpSpher C$_8$, 0.46 × 20 cm; Chrompack, Inc.). The solvents used were: solvent A, 0.1 M sodium citrate (pH 6.5), methanol (80:20, v/v); and solvent B, MeOH. The gradient (with t in minutes) was: t = 0, percent solvent B = 0; t = 19, percent solvent B = 0; t = 37, percent solvent B = 30; t = 45, percent solvent B = 45; and t = 55, percent solvent B = 60. This allowed good separation of tyrosine, alanine, and γ-aminobutyric acid. Each peak was collected and counted. Quantification was done from the peak area, determined by absorbance at 340 nm (Spectromonitor III, LDC/Milton Roy, Riviera Beach, FL), and response factors were determined by external standardization with the amino acid standard AA-S-18 (Sigma). The specificity of the peak area and radioactive counts of the aspartate and glutamate peaks was checked by HPLC analysis of the extract after enzymatic degradation of aspartate and glutamate in a medium (40 μl) containing the amino acid fraction corresponding to four embryos, 20 mM potassium phosphate (pH 7.4), 12 mM pyruvate, 0.025 mM pyridoxal phosphate, 0.75 mM NADH, and desalted enzymes (0.5 unit of alanine aminotransferase (EC 2.6.1.2), 0.1 unit of aspartate aminotransferase (EC 2.6.1.1), and 0.8 unit of malate dehydrogenase (EC 1.1.1.37)) and incubated for 1 h. These controls gave no evidence of either peak area or radioactivity extraneous to aspartate and glutamate.

Purification and Degradation of Glutamate—The remainder of the amino acid fraction was used for the purification of glutamic acid on Dowex 1 (CH$_3$COO$^-$) column with 0.5 M acetic acid using the procedure of Hirs *et al.* (1954). 2 μmol of glutamic acid were added as carrier. Recovery was close to 80%. The radioactivity of C-1 and C-5 in glutamate (O4 and A1, respectively, in the metabolic scheme (Fig. 1)) was determined after decarboxylation. The glutamate fraction was divided into two equal parts; C-5 was obtained by the Schmidt reaction according to Fuchs *et al.* (1980) and C-1 with glutamate decarboxylase (EC 4.1.1.15) using the procedure of Gale (1974). The amount of radioactivity in CO$_2$ and in the remaining carbons of glutamate was determined by counting the radioactivity in KOH and in the reaction medium. The yield of the two decarboxylation reactions, determined with standard [1-^{14}C]- and [5-^{14}C]glutamic acid, was 97 ± 1%. The ratio of the specific radioactivity of glutamate C-1 to that of glutamate C-5, S.R. O4/S.R. A1, was calculated as the ratio of the radioactivity in C-1 to the radioactivity in C-5.

Specific Radioactivity of Malate—The anionic fraction was evaporated to dryness, dissolved in 1 ml of water, adjusted to pH 7 ± 0.1, passed through a Sep-Pak C$_{18}$ cartridge (Waters Associates), which removed some radioactive contaminants of malate, and analyzed by HPLC according to Scharzenbach (1982). The radioactive contaminants still present in the malate fraction represented about 10% of

the radioactivity in malate as determined by two-dimensional thin-layer chromatography and autoradiography (Raymond *et al.*, 1985a). Malate was assayed enzymatically, the NADH being determined by bioluminescence (Golden and Katz, 1980).

THEORETICAL

The approach used is based on the assumption of isotopic and metabolic steady state, *i.e.* specific radioactivities and concentrations of the intermediates remain constant. The substrates were used at a tracer level and were assumed not to affect the metabolic state of the embryos. The concentrations of palmitate and hexanoate were below those reported to induce metabolic effects (Batayneh *et al.*, 1986; Ulbright *et al.*, 1982). The respiration rate and the level of adenine nucleotides increase slowly during the germination period, but slow changes in the level of some intermediates do not prevent application of a steady-state treatment (Borowitz *et al.*, 1977).

Metabolic Scheme—The metabolic scheme (Fig. 1) includes the tricarboxylic acid and glyoxylic cycles, with carbon input

FIG. 1. **Network of metabolic reactions used for simulation of embryo respiration at early stages of germination.** The terms under the carbon atoms denote the atoms of unique specific radioactivity. V_{GLYC}, glycolysis; V_{ASP}, synthesis of aspartate; V_{GLU}, synthesis of glutamate; V_{MAL}, reaction of malic enzyme; V_{PDH}, pyruvate dehydrogenase reaction; V_{PK}, pyruvate kinase reaction; V_{ACE}, CoASAc formation from acetate or fatty acids; V_{CS}, citrate synthase reaction; V_{KDH}, α-ketoglutarate dehydrogenase reaction; V_{GLYO}, input of succinate from the glyoxylate cycle; V_{FUM}, apparent flux from oxalacetate to fumarate; V_{FO}, apparent flux from fumarate to oxalacetate, $V_{FO} = V_{GLYO} + V_{KDH} + V_{FUM}$.

Respiratory Carbon Fluxes in Germinating Lettuce Embryos

from glycolysis or from fatty acid and amino acid degradation and carbon output to gluconeogenesis or amino acid synthesis. Malate and oxalacetate were treated as a single pool, as were citrate and isocitrate (Katz and Grunnet, 1979).

Carbon from glucose may enter the tricarboxylic acid cycle by two pathways. 1) After conversion to pyruvate by glycolysis, it may be metabolized by the pyruvate dehydrogenase reaction and incorporated as acetyl units at the level of citrate. 2) In plant cells, phosphoenolpyruvate may be carboxylated to oxalacetate by phosphoenolpyruvate carboxylase (EC 4.1.1.31), an enzyme which is widespread in plant tissues, including seeds (Latzko and Kelly, 1983). Oxalacetate can be reduced to malate; either compound may enter the tricarboxylic acid cycle.

The scheme includes three pathways of input of fatty acid carbon into the metabolism. These pathways are the following. 1) α-Oxidation oxidizes long-chain fatty acids to CO_2, which may enter the tricarboxylic acid cycle via the phosphoenolpyruvate carboxylase reaction. α-Oxidation has been demonstrated in germinated seeds (Shine and Stumpf, 1974). 2) The glyoxylate cycle utilizes the acetyl units formed by β-oxidation to produce succinate, which is oxidized in the tricarboxylic acid cycle (Cooper and Beevers, 1969; Galliard, 1980). It becomes very active at a relatively late stage of germination, but we did not exclude some low activity during the early stages studied here. Malate synthase activity has been found in a large number of dry seeds, including lettuce seeds (Miernyck and Trelease, 1979); and low isocitrate lyase activity has been found both in cotton seeds imbibed for 6 h (Smith *et al.*, 1974) and in sunflower seeds at the end of maturation and after 1 day of germination (Fusseder and Theimer, 1984). 3) The acetyl units produced by β-oxidation could be incorporated directly into the tricarboxylic acid cycle via citrate synthase. This pathway, which is well established in animals, has not been described in plants (Gerhardt, 1986).

Labeling of pyruvate from the malate + oxalacetate pool has been ascribed to a "malic" enzyme, but could also result from the sequence of the phosphoenolpyruvate carboxykinase and pyruvate kinase reactions, as described in animals (Rognstad and Katz, 1972). Amino acids in equilibrium with intermediates of the tricarboxylic acid cycle (Chance *et al.*, 1983) are also represented.

Carbon Fluxes—A first set of equations enables carbon fluxes to be calculated, so that for each compound, input equals output. The total carbon input (or output) has been normalized to input = 100. The model has 11 flux variables (shown in Fig. 1), and six flux parameters were used for the simulation: Fu, apparent rate of fumarase (FUM) expressed as a percentage of the net carbon flux from succinate to oxalacetate, $Fu = (V_{FUM}/(V_{GLYO} + V_{KDH})) \cdot 100$, where GLYO is glyoxylate cycle and KDH is α-ketoglutarate dehydrogenase; Ne, rate of gluconeogenesis (NEO) expressed as a percentage of the carbon output for biosyntheses, $Ne = 3 \cdot V_{NEO}/(input - V_{CO_2})) \cdot 100$; Ma, conversion of malate to pyruvate (MAL) expressed as a percentage of the flux of pyruvate carbon through the pyruvate dehydrogenase (PDH) reaction, $Ma = (V_{MAL}/V_{PDH}) \cdot 100$; Su, input of succinate from the glyoxylate cycle expressed as a percentage of the total input of carbon into the tricarboxylic acid cycle, $Su = (4 \cdot V_{GLYO}/input) \cdot 100$; Pe, input of carbon into the tricarboxylic acid cycle via the phosphoenolpyruvate carboxylase (PEPC)-catalyzed reaction expressed in relation to the rate of carbon input as acetyl units through the citrate synthase (CS) reaction, $Pe = (2 \cdot V_{PEPC}/V_{CS}) \cdot 100$; and Ac, non-glycolytic flux of acetyl units into the tricarboxylic acid cycle expressed in relation to the rate of carbon input as acetyl units (ACE)

Embryos were incubated with the labeled precursors for 6 h. The amount of radioactivity incorporated into carbohydrates and respiratory CO_2, measured as described under "Experimental Procedures," is expressed as a percentage of the total radioactivity incorporated. Results are the mean ± S.E.; *n* is the number of experiments.

Labeled precursor	Percentage of radioactivity incorporated recovered in:	
	Carbohydrates	CO_2
$^{14}CO_2$ ($n = 3$)	2.4 ± 0.5	
[U-^{14}C]Acetate ($n = 3$)	0.8 ± 0.1	20 ± 2
[U-^{14}C]Palmitate ($n = 3$)	<0.5	3 ± 1
[1-^{14}C]Hexanoate ($n = 5$)	3 ± 1	54 ± 6.5
[U-^{14}C]Glucose ($n = 5$)	9.5 ± 1.1	8.8 ± 0.1

through the citrate synthase reaction, $Ac = (V_{ACE}/V_{CS}) \cdot 100$.

Isotope Fluxes—The equations state that label inflow is equal to label outflow (Rognstad and Katz, 1972). The specific radioactivity of each unique carbon is calculated as a function of the rates and the specific radioactivities of its precursors. The specific radioactivities of the different compounds are then obtained by summing the specific radioactivities of their carbons. More detail on the treatment and resolution of the equations is given in the Miniprint.[2] The specific radioactivity of the labeled precursor has been normalized to 100. Except when $^{14}CO_2$ was the labeled precursor, the specific radioactivity of CO_2 was calculated by the model as a function of its precursors and rates. Validity of the resolution of the equations was checked with a mathematical solver, TK!Solver® (Universal Technical Systems, Rockford, IL). Calculations and simulations were made with a program written in Basic language in an MSDOS® environment. The specific radioactivity of the substrate carbons, a range of variation for the flux parameter chosen as the variable, and assumed values for the other fluxes were fed to the computer; specific radioactivity ratios were then calculated as a function of the rate variable. The value of the rate variable was determined from the experimental specific radioactivity ratio. The molar rates for the different reactions were then calculated using the rate of CO_2 evolution determined by manometry as described by Raymond *et al.* (1985a).

RESULTS

Establishment of Steady-state Conditions—Respiratory CO_2 (Table I) and organic and amino acids (Table II) were labeled with all the substrates used. The labeling with acetate and glucose has been described previously (Raymond *et al.*, 1985a). Palmitate and hexanoate were rapidly taken up from the medium; the fraction converted to CO_2 was smaller with palmitate than with hexanoate, thus indicating a much lower catabolism of the long-chain fatty acid, which was incorporated mainly in the lipid fraction (data not shown). With all three fatty acids, there was some incorporation of label into carbohydrates. The carbon flux into gluconeogenesis was much lower than into CO_2 (Table I).

The kinetics of labeled CO_2 evolution were determined to check the establishment of steady state. At steady state, the labeling of CO_2 should become linear (Borowitz *et al.*, 1977).

---

[2] Portions of this paper (including "Calculation of the Carbon Flux," "Steady-state Equations for Isotope Inflow and Outflow," Equations 1–19 and 1'–8', additional Equations 1–15, and Matrices 1 and 2) are presented in miniprint at the end of this paper. Miniprint is easily read with the aid of a standard magnifying glass. Full size photocopies are included in the microfilm edition of the Journal that is available from Waverly Press.

TABLE II

Specific radioactivities of aspartate, glutamate, alanine, and malate after 6 h of labeling with different ^{14}C-substrates

Embryos were incubated with the labeled precursors for 6 h. Specific radioactivities were determined after HPLC analysis of amino acids and bioluminescence assay after HPLC separation of malate, as described under "Experimental Procedures." Specific radioactivities are the mean ± S.E. of n determinations.

Labeled precursor	Specific radioactivities			
	Aspartate	Glutamate	Alanine	Malate
	$dpm \cdot nmol^{-1}$			
$^{14}CO_2$ ($n = 6$)	505 ± 15	300 ± 6	96 ± 10	569 ± 54
[U-^{14}C]Acetate ($n = 5$)	64 ± 7	83 ± 6	19 ± 6	
[U-^{14}C]Palmitate ($n = 3$)	9.9 ± 1.1	12.9 ± 1.1	2.7 ± 0.1	
[1-^{14}C]Hexanoate ($n = 5$)	632 ± 110	871 ± 146	27 ± 1	677 ± 143
[U-^{14}C]Glucose ($n = 6$)	158 ± 18	156 ± 11	290 ± 33	

Incubation time (h)
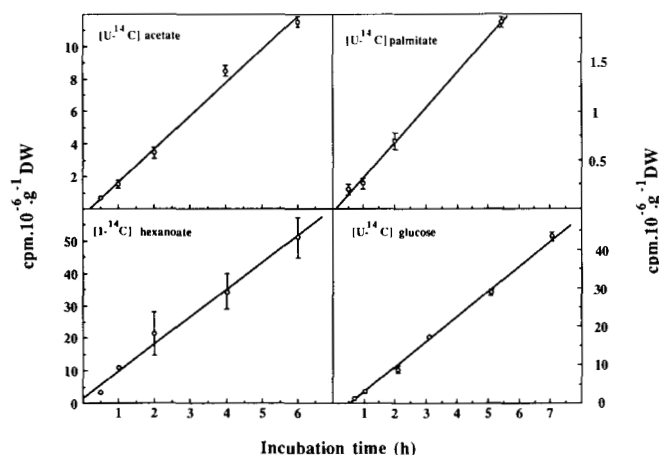
FIG. 2. **Time course of radioactive CO_2 evolution during labeling with [U-^{14}C]acetate, [U-^{14}C]palmitate, [1-^{14}C]hexanoate, and [U-^{14}C]glucose.** Embryos were incubated with the labeled precursors for various times, and respiratory CO_2 was collected as indicated under "Experimental Procedures." The amount of radioactivity incorporated in respiratory CO_2 is corrected for blank values (radioactivity found in the absence of embryo). Results are the mean ± S.E. of determination in two experiments with duplicate samples. The correlation coefficients of the regression lines were higher than 0.99. *DW*, dry weight.

With [U-^{14}C]glucose, there was a lag of about 30 min before linearity was reached; with [U-^{14}C]acetate, the lag was only about 15 min; and no lag was detected with [1-^{14}C]acetate, [1-^{14}C]hexanoate, or [U-^{14}C]palmitate (Fig. 2). However, since compartmentalized pools may reach isotopic steady state more slowly than those directly connected to the tricarboxylic acid cycle, the labeling time used was 6 h. With [1-^{14}C] hexanoate and [U-^{14}C]glucose, we verified that the S.R. Asp/ S.R. Glu ratio was the same after 4 and 6 h of labeling.

Specific Radioactivities at Steady State—The specific radioactivities of the different compounds analyzed (Table II) vary by 2 orders of magnitude depending on the precursor used, with low values after palmitate labeling and high values after $^{14}CO_2$ and [1-^{14}C]hexanoate labeling. These differences are not related to the specific radioactivity or amount of precursor and seem to reflect different dilutions by endogenous substrates. The determination of the specific radioactivity of malate was hampered by high variability, which could be due to variability in radioactive contaminations or in the enzymatic determinations, and only the results obtained after

$^{14}CO_2$ and [1-^{14}C]hexanoate labeling are shown; the specific radioactivities of aspartate and malate are close to each other. This is in agreement with the assumption of the model that malate and aspartate reflect the specific radioactivity of oxalacetate.

The steady-state model was used to determine most of the flux parameters; the rate of gluconeogenesis and complementary information on the pathway of fatty acid degradation were obtained in non-steady-state conditions.

Apparent Fumarase Rate—The labeling of malate and aspartate (Table II) and the specific labeling of O4 in glutamate with $^{14}CO_2$ (Table III) indicate the operation of the phosphoenolpyruvate carboxylase reaction. Labeling of intermediates with $^{14}CO_2$ is very sensitive to the flux through the fumarase reaction, which randomizes O1 and O4 (Fig. 3); since both O1 and O4 are present in aspartate and only O4 remains in glutamate, the S.R. Asp/S.R. Glu ratio may vary from 1 (no randomization; Fu = 0) to 2 (complete randomization; for Fu = 1000, S.R. Asp/S.R. Glu = 1.83). The relative labeling of aspartate and glutamate with $^{14}CO_2$ was used to determine the fumarase parameter, Fu. The determination of Fu is little affected by variations of the flux through the

TABLE III

Distribution of radioactivity in glutamate after labeling with $^{14}CO_2$, [1-^{14}C]hexanoate, and [U-^{14}C]glucose

Embryos were labeled for 6 h, and glutamate was analyzed as indicated under "Experimental Procedures." O4 is glutamate C-1, and A1 is glutamate C-5. Results are the mean ± S.E. of n determinations. If $^{14}CO_2$ entered the tricarboxylic acid cycle via the phosphoenolpyruvate carboxylase, 100% of the label in glutamate should be located at O4; the theoretical label distribution, when [1-^{14}C] hexanoate is degraded via β-oxidation and enters the tricarboxylic acid cycle via citrate synthase, is 33% of O4 and 67% at A1.

Labeled precursor	Percentage of glutamate radioactivity in:		
	O4	A2 + O-2 + O-3	A1
$^{14}CO_2$ ($n = 6$)	94.7 ± 1	1.2 ± 1	4.1 ± 2
[1-^{14}C]Hexanoate ($n = 5$)	27.8 ± 0.2	2 ± 2	71 ± 1
[U-^{14}C]Glucose ($n = 11$)	21 ± 2	73.4 ± 3	5.6 ± 1

$$Fu = \frac{V_{FUM}}{V_{GLY} + V_{KDH}} \cdot 100$$
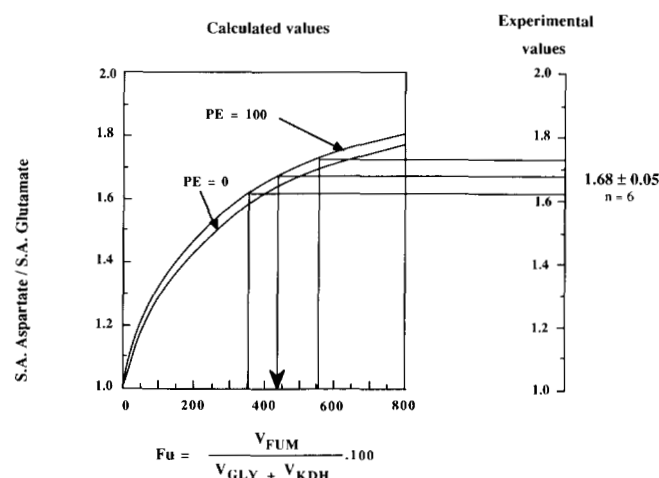
FIG. 3. **Determination of apparent fumarase rate from S.R. Asp/S.R. Glu ratio.** The curves show the theoretical values of S.R. Asp/S.R. Glu as a function of Fu, the relative rate of the reverse reaction of fumarase, for two values of Pe. Determination of experimental values of S.R. Asp/S.R. Glu was performed as described under "Experimental Procedures" after labeling lettuce embryos for 6 h with $^{14}CO_2$. Determination of Fu values corresponding to the experimental data is shown.

TABLE V

Incorporation of radioactivity into citrate, malate, aspartate, and glutamate during short-term labeling with [1-^{14}C]hexanoate

Samples of 20 embryos were incubated for 1–10 min with [1-^{14}C] hexanoate (74 KBq). The amounts of radioactivity in the different organic and amino acids and the specific radioactivities of amino acids were determined as described under "Experimental Procedures." The percentages of radioactivity of the anionic fraction recovered in citrate and malate and of the cationic fraction recovered in aspartate and glutamate are in parentheses. Variability of the amount of radioactivity recovered was within 15% of the mean ($n = 4$).

Compound	Time of incubation			
	1 min	2 min	5 min	10 min
	dpm·g dry weight^{-1}·10^{-3}			
Radioactivity of:				
Citrate	101.5	164	296	391
	(63)	(56)	(44)	(32)
Malate	10.5	23.5	78.5	308
	(7)	(8)	(12)	(25)
Glutamate	71	151	670	1275
	(86)	(86)	(84)	(68)
Aspartate	6.5	19	72	392
	(9)	(10)	(11)	(21)
	dpm/nmol			
Specific radioactivity of:				
Aspartate	3.5 ± 0.3	10 ± 1	39 ± 1	225 ± 6
Glutamate	28	57 ± 2	224 ± 23	641 ± 15

This sequence indicates a metabolism by the tricarboxylic acid cycle rather than the glyoxylate cycle. In castor bean endosperm supplied with labeled acetate (Canvin and Beevers, 1961), malate was more labeled than citrate after a short period of labeling and over the whole labeling period, and this was consistent with the operation of the glyoxylate cycle. We conclude from this experiment that the glyoxylate cycle is not operative and that the anaplerotic input of carbon is due to the phosphoenolpyruvate reaction.

Contribution of Carbohydrates to the Flux of Acetyl Units into the Tricarboxylic Acid Cycle—In an attempt to determine the relative contribution of carbohydrates or fatty acids to the flux of CoASAc entering the tricarboxylic acid cycle, we compared the specific radioactivity of the carbons derived from CoASAc (A1 and A2) to that of the carbons of oxalacetate (O1 to O4) after labeling with [U-^{14}C]glucose. All these carbons would have the same specific radioactivity if they were formed from the carbohydrate pool labeled with [U-^{14}C] glucose, but the relative specific radioactivities of A1 and A2 should be decreased by a flux of CoASAc from an endogenous unlabeled source entering the tricarboxylic acid cycle via citrate synthase. Simulations showed that the label distribution is very sensitive to Ac (dilution of the labeled CoASAc from glucose by unlabeled CoASAc) and, to a lesser extent, to Pe. Variations of the S.R. Asp/S.R. Glu and S.R. A1/S.R. O4 ratios as functions of Ac are shown in Fig. 4. The specific radioactivities of aspartate and glutamate had similar values (S.R. Asp/S.R. Glu = 1.01 ± 0.1; Table II), and A1 in glutamate was less labeled than O4 (S.R. A1/S.R. O4 = 0.23 ± 0.01). These results indicate that A1 and A2 are less labeled than O1 to O4, which derive, in part, from the carboxylation of phosphoenolpyruvate. The values of Ac corresponding to the experimental results indicate that the labeled carbohydrates contribute less than 10% to the total CoASAc flux entering the tricarboxylic acid cycle. Increasing Pe has the effect of increasing the relative labeling of aspartate and produces the same effect on the S.R. Asp/S.R. Glu ratio as a dilution of the radioactivity of the acetyl units. However, even for Pe = 50, a value of the carbon flux through the phosphoen-

Calculated values   Experimental values

$$Ac = \frac{V_{ACE}}{V_{CS}} \cdot 100$$

FIG. 4. **Determination of Ac, contribution of unlabeled carbon to flux of CoASAc into tricarboxylic acid cycle.** Theoretical S.R. Asp/S.R. Glu (*upper*) and S.R. A1/S.R. O4 (*lower*) values were calculated as described in the Miniprint by a simulation of the [U-^{14}C]glucose labeling experiment using Pe = 20, Fu = 430, Ma = 15, Su = 0, and Ne = 51. Lettuce embryos were labeled with [U-^{14}C] glucose for 6 h; the determination of the experimental specific radioactivity of aspartate and glutamate was obtained after HPLC analysis of the amino acids, and the S.R. A1/S.R. O4 ratio by decarboxylations of glutamate as described under "Experimental Procedures." The Ac values corresponding to the experimental S.R. Asp/S.R. Glu (*upper*) and S.R. A1/S.R. O4 (*lower*) ratios are shown.

olpyruvate carboxylase reaction higher than the limit indicated by the acetate and palmitic acid labeling, Ac remains as high as 80%; the labeled carbohydrates contribute only 20% to the CoASAc flux into the tricarboxylic acid cycle. These results indicate that most of the acetyl units are formed from an endogeneous unlabeled source and that the flux of labeled carbohydrates through the phosphoenolpyruvate carboxylase reaction is higher than through the pyruvate dehydrogenase reaction (Table VI).
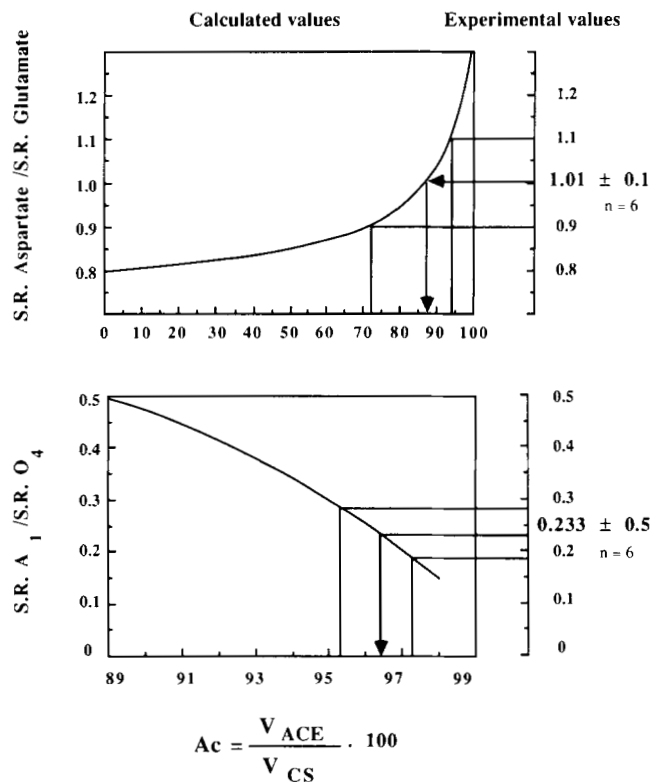
Gluconeogenesis—The carbon flux in gluconeogenesis was calculated after labeling with ^{14}CO$_2$ and [1-^{14}C]hexanoate from the amount of radioactivity incorporated in the neutral fraction (Table I) and the specific radioactivity of O1, the only labeled carbon incorporated into carbohydrates. It was assumed that incorporation was linear with time and that the radioactivity output by glycolysis was negligible. If gluconeogenesis labels the same carbohydrate pool that is used by glycolysis, this assumption remains valid as long as the specific radioactivity of the carbohydrate pool is low compared to that of O1, but it leads to an underestimation of gluconeogenesis when the labeling of carbohydrates increases. The molar rate of gluconeogenesis was calculated as follows: V_{NEO} = rate of carbohydrate labeling × 3/S.R. O1. After labeling with ^{14}CO$_2$, incorporation of radioactivity into carbohydrates was 115,000 dpm·h^{-1}·g^{-1}; the specific radioactivity of O1 was calculated assuming that S.R. Asp = S.R. O1 + S.R. O4 and S.R. Glu = S.R. O4 and using the specific radioactivity values

TABLE VI

Calculated values of steady-state metabolic fluxes

The rates in μmol of carbon$\cdot$h$^{-1}\cdot$g^{-1} dry weight are those mentioned in Fig. 1. They have been calculated from the flux parameter giving the best fit to experimental data and from the independent determination of V_{CO_2} (obtained by determination of the CO_2 evolution by manometry). The production of CO_2 from other pathways (*i.e.* the pentose phosphate pathway) was neglected; this may lead to an overestimation of the rates, but does not affect their values in relation to each other.

Flux parameter	Relative value	Range of variation	Carbon flux	Absolute value
				$\mu mol\ C\cdot h^{-1}\cdot g^{-1}$
$Ac = (V_{ACE}/V_{CS})\cdot 100$	95	3	$2\cdot V_{ACE}$	30
$Pe = (2\cdot V_{PEPC}/V_{CS})\cdot 100$	20	10	$3\cdot V_{PEPC}$	4.7
$Su = (4\cdot V_{GLYO}/input)\cdot 100$	0	0	$4\cdot V_{GLYO}$	0
$Fu = (V_{FUM}/(V_{GLY} + V_{KDH}))\cdot 100$	430	100	$4\cdot V_{FUM}$	260
$Ma = (V_{MAL}/V_{PDH})\cdot 100$	15	30	$4\cdot V_{MAL}$	0.4
$Ne = (3\cdot V_{NEO}/(input - V_{CO_2}))\cdot 100$	51	16	$4\cdot V_{NEO}$	3.3
			$3\cdot V_{PDH}$	2.6
			$3\cdot V_{PK}$	2.2

$$V_{CO_2} = 33\ \mu mol\ C\cdot h^{-1}\cdot g^{-1}$$

given in Table II. After labeling with [1-^{14}C]hexanoate, the incorporation of radioactivity into carbohydrates was 330,000 dpm$\cdot$h$^{-1}\cdot$g^{-1}, and S.R. O1 was calculated from S.R. Glu and S.R. Asp assuming that the label of A1 was equally distributed between O1 and O4; from S.R. Asp = 632, we calculated S.R. O1 = 316 and from S.R. Glu = 871, S.R. O1 = 290. The mean value of these two determinations of the carbon input into carbohydrates is $3\cdot V_{NEO} = 2.5 \pm 0.8$ μmol of carbon$\cdot$h$^{-1}\cdot$g^{-1}. This gluconeogenesis flux is 7.4 $\pm$ 2% of the respiratory CO_2. Table VI shows the derivation of carbon from the tricarboxylic acid cycle to gluconeogenesis ($4\cdot V_{NEO}$).

DISCUSSION

The monocompartmental model used in the study is evidently a great simplification of the metabolic pathways studied. However, the agreement between the relative specific radioactivities in the couples aspartate/glutamate and A1/O4 glutamate as well as the possibility of fitting the model with data from different precursors indicate that the model is adequate for detecting and quantifying carbon fluxes in some of the metabolic pathways studied.

There is only limited evidence for the existence of some of the enzymes of the tricarboxylic acid cycle in germinating seeds or for the operation of this pathway *in vivo* (Bewley and Black, 1985). Our results showing the relative labeling of aspartate and glutamate with [U-^{14}C]acetate and the pattern of glutamate labeling with ^{14}CO$_2$ and [1-^{14}C]hexanoate are consistent with the operation of the complete tricarboxylic acid cycle.

The apparent fumarase reaction rate (Fig. 3) was determined after labeling with ^{14}CO$_2$; the value of Fu = 430 $\pm$ 100 (Fig. 3) determined from the experimental S.R. Asp/S.R. Glu ratio of 1.68 $\pm$ 0.06 is of the order of that determined in animal tissues: Fu = 1200 in kidney cortex (Rognstad and Katz, 1972) and Fu = 400 in myocardium (Nuutinen *et al.*, 1981). The distribution of label between O1 and O4 is consistent with the O1/O4 ratio found in different plant tissues after labeling with ^{14}CO$_2$ (Levi *et al.*, 1978; Popp *et al.*, 1982) and with the active labeling of carbon 1 of malate or aspartate in marrow cotyledons (Leegood and ap Rees, 1978). Since phosphoenolpyruvate carboxylase is localized in the cytosol of all plant tissues studied, the fumarase rate determined in this way is not that of the mitochondrial reaction only, but includes the rate of exchange of malate or oxalacetate between the different cellular compartments.

The labeling of organic and amino acids with [U-^{14}C]glucose indicates the operation of glycolysis. The occurrence of the phosphoenolpyruvate carboxylase reaction was shown with ^{14}CO$_2$ by the labeling of malate and aspartate and by the specific labeling of O4 in glutamate (Table III). When labeling with [U-^{14}C]glucose, this reaction accounted for the higher specific radioactivity of the glutamate molecule of the carbons from oxalacetate compared to those from CoASAc.

Gluconeogenesis has been detected here with [U-^{14}C]acetate, ^{14}CO$_2$, and [1-^{14}C]hexanoate labeling. With [U-^{14}C]acetate, the relative amounts of label in carbohydrates and CO_2 after 6 h (3/30%) were similar to those found after 1 h (Raymond *et al.*, 1985a). With [1-^{14}C]hexanoate, the labeling of CO_2 was 20 times greater than that of carbohydrates. This relatively low activity of gluconeogenesis contrasts with that observed in castor bean endosperm when the glyoxylate cycle operates (Canvin and Beevers, 1961); with [1-^{14}C]acetate, the labeling of carbohydrates was close to that of CO_2, and with [2-^{14}C]acetate, the labeling of CO_2 was extremely low. In marrow cotyledons, on the first day of germination, similar amounts of label from [2-^{14}C]acetate were incorporated into CO_2 and carbohydrates (Thomas and ap Rees, 1972). In germinating lettuce embryos, the catabolism of fatty acids in the tricarboxylic acid cycle predominates over gluconeogenesis.

The simultaneous operation of glycolysis and gluconeogenesis has been described in animals (for example, see Rognstad and Katz, 1972) and in plants (in the cotyledons of germinating marrow seed (Thomas and ap Rees, 1972) and in the endosperm of castor bean (Kobr and Beevers, 1971)); it also occurs in lettuce embryos. The rate of glycolysis, calculated as the sum of V_{PEPC} and V_{PK} (where PK is pyruvate kinase), determined by fitting of the model, is 6.9 μmol of carbon$\cdot$h$^{-1}\cdot$g^{-1} (Table VI). This result agrees with an independent estimate of the maximum rate of glycolysis in lettuce seeds as the rate of accumulation of ethanol and lactate under anoxia, which was close to 12 μmol of carbon$\cdot$h$^{-1}\cdot$g^{-1} (Raymond *et al.*, 1985b). However, it remains an imprecise estimation of the aerobic rate of glycolysis.

The rate of gluconeogenesis has been quantified after ^{14}CO$_2$ and [1-^{14}C]hexanoate labeling from the derivation of radioactivity into sugars and the specific radioactivity of O1. Since the labeling of the ester phosphates and of insoluble polysaccharides has been neglected, the value of $3\cdot V_{NEO} = 2.5 \pm 0.8$ μmol of carbon$\cdot$h$^{-1}\cdot$g^{-1} is a minimum rate of gluconeogenesis.

It is very close to that of glycolysis, which does, however, seem to predominate. This situation contrasts with that found in castor bean endosperm; Kobr and Beevers (1971) found that the maximum rate of glycolysis was only one-tenth of the gluconeogenic rate during gluconeogenesis. More detailed studies in lettuce embryos are required to establish if the two pathways operate in the same tissue or cellular compartment, as a futile cycle, or if they are compartmentalized. The excess of V_{PEPC} over $V_{NEO} + V_{MAL}$ is accounted for by the model as a net synthesis of amino acids.

Evidence that fatty acids are degraded by β-oxidation has been obtained with two fatty acids labeled in different positions: [U-^{14}C]palmitate and [1-^{14}C]hexanoate. The very efficient degradation of hexanoate to CO_2 is in favor of β-oxidation since the α-oxidation systems of other plant tissues do not utilize short chain fatty acids (Galliard, 1980). The relative labeling of aspartate and glutamate and of A1 and O4 indicates that the acetyl units produced by β-oxidation enter the tricarboxylic acid cycle at the citrate synthase step. Most studies on β-oxidation in plants have been performed on growing seedlings after germination; β-oxidation is generally associated with the synthesis of carbohydrates via the glyoxylate cycle. Its role in the direct supply of carbon to respiration has not previously been demonstrated. As regards its subcellular localization, the β-oxidation system has been demonstrated unambiguously only in plant peroxisomes and glyoxysomes, and although it has often been assumed to be present in mitochondria, the experimental evidence was not considered conclusive (Gerhardt, 1986). Citrate synthase, on the contrary, is found both in peroxisomes (or glyoxysomes) and in mitochondria (Miernyck and Trelease, 1981; Cooper and Beevers, 1969). Although our results suggest a close relationship between β-oxidation and the tricarboxylic acid cycle, it should be noted that they provide no indication of the intracellular localization of the different reactions.

The [U-^{14}C]glucose labeling experiment showed that glucose contributes little to the formation of CoASAc. This is only an indirect indication that fatty acids could be the major source of acetyl units. However, among the potential substrates, which may be carbohydrates, amino acids, or fatty acids, the latter appear to be the most likely.

If the source of unlabeled acetyl units is an unlabeled pool of carbohydrates, it should be degraded to pyruvate by a compartmentalized glycolysis, and the labeling of pyruvate should be low. This is not consistent with the high specific radioactivity of alanine (Table II). We conclude that oxalacetate and the labeled acetyl units are formed from the same carbohydrate pool. The determination of Pe and Ac (Table VI) makes it possible to calculate that 70% of the glycolytic flux is metabolized by phosphoenolpyruvate carboxylase compared with only 30% by pyruvate kinase. Such a partition of the glycolytic flux is in agreement with data obtained in different higher plant materials which show that both oxalacetate and pyruvate are end products of glycolysis (Davies, 1979).

The degradation of endogenous amino acids would introduce unlabeled carbon not only at the level of CoASAc, but at many other steps of the tricarboxylic acid cycle (ap Rees, 1980), and would decrease the specific radioactivity of all intermediates rather than, specifically, that of the acetyl units in CoASAc.

Therefore, although fatty acids are not considered a quantitatively important respiratory substrate in plant cells (ap Rees, 1980), they appear to be the most likely source in germinating lettuce embryos. This is suggested by: 1) the pattern of steady-state labeling of the tricarboxylic acid cycle intermediates with ^{14}C-labeled fatty acids, which indicates that exogenous fatty acids are degraded by β-oxidation and that their carbon is incorporated at the level of citrate; 2) the high rate of labeled CO_2 evolution compared to that of gluconeogenesis when labeling with ^{14}C-fatty acids; 3) the sequence of labeling of intermediates with [1-^{14}C]hexanoate, which gave no evidence for the operation of the glyoxylate cycle; and 4) the low contribution of glucose to the formation of CoASAc.

This hypothesis is sustained by independent results. 1) The respiratory quotient of lettuce seeds and embryos (Raymond *et al.*, 1985a) corresponds to the respiration of fatty acids. 2) In germinating seeds of sunflower (which belongs to the same family as lettuce, the Compositae), the ^{13}C/^{12}C ratio of the respiratory CO_2 also indicated that CO_2 arises from lipids (Smith, 1971). 3) The low contribution of glycolysis to the respiratory flux of carbon, and particularly the low flux through the pyruvate kinase branch of glycolysis, is consistent with the low fermentative activity found in germinating lettuce seeds as well as in other fat-storing seeds (Raymond *et al.*, 1985b).

REFERENCES

ap Rees, T. (1980) in *The Biochemistry of Plants* (Davies, D. D., ed) Vol. 2, pp. 1–29, Academic Press, New York
Batayneh, N., Kopacz, S. J., and Lee, C. P. (1986) *Arch. Biochem. Biophys.* **250**, 476–487
Bewley, J. D., and Black, M. (1985) *Seeds: Physiology of Development and Germination*, Plenum Publishing Corp., New York
Borowitz, M. J., Stein, R. B., and Blum, J. J. (1977) *J. Biol. Chem.* **252**, 1589–1605
Burbach, J. P. H., Prins, A., Lebouille, J. L. M., Verhoef, J., and Witter A. (1982) *J. Chromatogr.* **237**, 339–343
Canvin, D. T., and Beevers, H. (1961) *J. Biol. Chem.* **236**, 988–995
Chance, E. M., Seeholzer, S. H., Kobayashi, K., and Williamson, J. R. (1983) *J. Biol. Chem.* **258**, 13785–13794
Connett, R. J., and Blum, J. J. (1971) *Biochemistry* **10**, 3299–3309
Cooper, T. G. and Beevers, H. (1969) *J. Biol. Chem.* **244**, 3507–3513
Crowe, J. H., Crowe, L. M., Carpenter, J. F., and Aurell Wistrom, C. (1987) *Biochem. J.* **242**, 1–10
Davies, D. D. (1979) *Annu. Rev. Plant Physiol.* **30**, 131–158
Fuchs, G., Stupperich, E., and Eden, G. (1980) *Arch. Microbiol.* **128**, 64–71
Fusseder, A., and Theimer, R. R. (1984) *Z. Pflanzenphysiol.* **114**, 403–411
Gale, E. (1974) in *Methods in Enzymatic Analysis* (Bergmeyer, H. U., ed) Vol. 4, pp. 1662–1668, Academic Press, New York
Galliard, T. (1980) in *The Biochemistry of Plants* (Stumpf, P. K., and Conn, E. E., eds) Vol. 7, pp. 85–116, Academic Press, New York
Gerhardt, B. (1986) *Physiol. Veg.* **24**, 397–410
Golden, S., and Katz, J. (1980) *Biochem. J.* **188**, 799–805
Hirs, C., Moore, S., and Stein, W. (1954) *J. Am. Chem. Soc.* **76**, 6063
Hourmant, A., and Pradet, A. (1981) *Plant Physiol.* **68**, 631–635
Katz, J., and Grunnet, N. (1979) *Techn. Metab. Res.* **208**, 1–18
Kobr, M. J., and Beevers, H. (1971) *Plant Physiol.* **47**, 48–52
Latzko, E., and Kelly, G. J. (1983) *Physiol. Veg.* **21**, 805–815
Leegood, R. C., and ap Rees, T. (1978) *Planta (Berl.)* **140**, 275–282
Levi, C., Perchorowicz, J. T., and Gibbs, M. (1978) *Plant Physiol.* **61**, 477–480
Mayer, A. M., and Poljakoff-Mayber, A. (1963) in *The Germination of Seeds* (Wareing, P. F., and Galston, A. W., eds) Vol. 3, pp. 85–116, Pergamon Press, New York
Miernyck, J. A., and Trelease, R. N. (1979) *Plant Physiol.* **63**, 1068–1071
Miernyck, J. A., and Trelease, R. N. (1981) *Plant Physiol.* **67**, 875–881
Nuutinen, E. M., Peuhkurinen, K. J., Pietilainen, E. P., Hiltunen, J. K., and Hassinen, I. E. (1981) *Biochem. J.* **194**, 867–875
Popp, M., Osmond, C. B., and Summons, R. E. (1982) *Plant Physiol.* **69**, 1289–1292
Raymond, P., and Pradet, A. (1980) *Biochem. J.* **190**, 39–44

Raymond, P., Carre-Nemesio, A. M., and Pradet, A. (1985a) *Physiol. Plant* **64**, 529–534

Raymond, P., Al-Ani, A., and Pradet, A. (1985b) *Plant Physiol.* **71**, 875–884

Rognstad, R., and Katz, J. (1972) *J. Biol. Chem.* **247**, 6047–6054

Schwarzenbach, R. (1982) *J. Chromatogr.* **251**, 339–358

Shine, W. E., and Stumpf, P. K. (1974) *Arch. Biochem. Biophys.* **162**, 147–157

Smith, B. N. (1971) *Plant Cell Physiol.* **12**, 451–455

Smith, R. H., Schubert, A. M., and Benedict, C. R. (1974) *Plant Physiol.* **54**, 197–200

Stitt, M., and ap Rees, T. (1978) *Phytochemistry (Oxf.)* **17**, 1251–1256

Thomas, S. M., and ap Rees, T. (1972) *Phytochemistry (Oxf.)* **11**, 2187–2194

Ulbright, C. E., Pickard, B. G., and Varner, J. E. (1982) *Plant Cell Environ.* **5**, 293–301

Supplemental Material to :
Quantification of carbon fluxes through the tricarboxylic acid cycle in early germinating lettuce embryos

Christophe Salon, Philippe Raymond and Alain Pradet.

I Calculation of the carbon flux

The model calculates at first the molar rates of the metabolic scheme according to the steady state assumptions.

1) **Definitions.** We have chosen reference rates for the simulations and for simplifying the algebra :

V_{ACE} (Input of non glycolytic acetate in the CoASAc pool)
V_{GLYO} (Input of glyoxosomal succinate in the succinate pool)
V_{MAL} (Flux through the malic enzyme)
V_{KDH} (Flux through the α-ketoglutarate dehydrogenase)
V_{ASP} (Synthesis of aspartate)
V_{PEPC} (Flux through the phosphoenolpyruvate carboxylase)
V_{NEO} (Flux to neoglucogenesis)

2) **Calculation of rates.** The rates are defined in fig. 1. In the steady state, the flow into a compound must equal the flow out of it so all these rates are not independent. For example the rates of pyruvate formation from phosphoenolpyruvate and malate must equal the rate of loss of pyruvate to acetyl-CoA and it can be written: $V_{PK} + V_{MAL} = V_{PDH}$
For each node a similar equation is written.

Node	Equation	
phosphoenolpyruvate	$V_{GLYC} = V_{PK} + V_{PEPC}$	(1)
Pyruvate	$V_{PK} + V_{MAL} = V_{PDH}$	(2)
CoASAc	$V_{ACE} + V_{PDH} = V_{CS}$	(3)
Oxoglutarate	$V_{CS} = V_{KDH} + V_{GLU}$	(4)
Fumarate	$V_{FUM} + V_{GLYO} + V_{KDH} = V_{FO}$	(5)
Oxaloacetate	$V_{FO} + V_{PEPC} = V_{ASP} + V_{FUM} + V_{NEO} + V_{MAL} + V_{CS}$	(6)

Glyoxylate cycle : All rates in the glyoxylate cycle are equal to the rate of glyoxylic acid input into this cycle.

The other rates (V_{CS} , flux through citrate synthase ; V_{PDH} , flux through pyruvat dehydrogenase ; V_{GLU} , net output of glutamate ; V_{PK} , flux through pyruvate kinase ; V_{GLYC} , entry of glucose via the glycolysis, V_{FUM} , flux through fumarase) are expressed as a function of the reference ones.

Substituting (5) into (6) yields :

$V_{CS} = V_{KDH} + V_{PEPC} + V_{GLYO} - V_{MAL} - V_{NEO} - V_{ASP}$ (7)

Then introducing (7) into (3) to obtain V_{PDH} and (7) into (4) to give V_{GLU}

$V_{PDH} = V_{KDH} + V_{PEPC} + V_{GLYO} - V_{MAL} - V_{NEO} - V_{ASP} - V_{ACE}$ (8)
$V_{GLU} = V_{PEPC} + V_{GLYO} - V_{MAL} - V_{NEO} - V_{ASP}$ (9)

Next substituting equation (8) into (2)

$V_{PK} = V_{KDH} + V_{PEPC} + V_{GLYO} - 2 \cdot V_{MAL} - V_{NEO} - V_{ASP} - V_{ACE}$ (10)

and finally, substituting (10) into (1)

$V_{GLYC} = V_{KDH} + 2 \cdot V_{PEPC} + V_{GLYO} - 2 \cdot V_{MAL} - V_{NEO} - V_{ASP} - V_{ACE}$ (11)

3) **Normalization of rates.** Furthermore, the values of the reference rates must be introduced for the resolution of the system, they were calculated as follow :

3.1. The total input of carbon into the cycle and the total output of carbon were normalised, giving the equations :

INPUT = OUTPUT = 100
INPUT = $4 \cdot V_{GLYO} + 3 \cdot V_{GLYC} + 2 \cdot V_{ACE} + V_{PEPC}$
OUTPUT = $3 \cdot V_{NEO} + 5 \cdot V_{GLU} + 4 \cdot V_{ASP} + V_{NEO} + V_{MAL} + V_{PDH} + V_{CS} + V_{KDH}$

Expressing all rates as a function of the reference rates leads to the equation :

$3 \cdot V_{KDH} + 7 \cdot V_{PEPC} + V_{GLYO} - 6 \cdot V_{MAL} - 3 \cdot V_{NEO} - 3 \cdot V_{ASP} - V_{ACE} = 100$ (12)

3.2. The input of carbon into the T.C.A cycle via the glyoxylate cycle was expressed as a percentage Su (0 ≤ Su ≤ 1) of the total input of carbon.

$4 \cdot V_{GLYO} = Su.INPUT$

hence

$Su \cdot (3 \cdot V_{KDH} + 7 \cdot V_{PEPC} - 6 \cdot V_{MAL} - 3 \cdot V_{NEO} - 3 \cdot V_{ASP} - V_{ACE}) + (7.Su-4) \cdot V_{GLYO} = 0$ (13)

3.3. The synthesis of glutamate and that of aspartate were expressed as percentages (Gl and As, resp.) of the output of carbon available for biosynthesis i.e total output of carbon minus the evolved CO2.

CO_2 evolved = $V_{NEO} + V_{MAL} + V_{PDH} + V_{CS} + V_{KDH}$

substituting the value of V_{CS} and V_{PDH} into this equation leads to :

CO_2 evolved = $3 \cdot V_{KDH} + 2 \cdot V_{PEPC} + 2 \cdot V_{GLYO} - V_{MAL} - V_{NEO} - V_{ACE} - 2 \cdot V_{ASP}$
Carbon available = INPUT - CO_2 evolved
= $5 \cdot V_{PEPC} + 5 \cdot V_{GLYO} - 5 \cdot V_{MAL} - 2 \cdot V_{NEO} - V_{ASP}$

hence, the synthesis of glutamate and aspartate can be expressed as :

$5 \cdot V_{GLU} = Gl \cdot$ Carbon available
$0 = Gl.(5.V_{PEPC} + 5.V_{GLYO} - 5.V_{MAL} - 2.V_{NEO} - V_{ASP}) - 5.V_{GLU}$ (14)
$4 \cdot V_{ASP} = As \cdot$ Carbon available
$0 = As.(5.V_{PEPC} + 5.V_{GLYO} - 5.V_{MAL} - 2.V_{NEO}) - (As+4).V_{ASP}$ (15)

3.4. Neoglucogenesis was expressed as a percentage of the CO2 available.

$3 \cdot V_{NEO} = Ne \cdot$ Carbon available
$0 = Ne.(5.V_{PEPC} + 5.V_{GLYO} - 5.V_{MAL} - V_{ASP}) - (2.Ne+3).V_{NEO}$ (16)

3.5. The contribution of glucose and fatty acid acetyl units was expressed relatively to the total flux of acetyl-units entering the tricarboxylic acid cycle via the citrate synthase catalysed reaction :

$2 \cdot V_{ACE} = 2.Ac.V_{CS}$
$0 = Ac.(V_{KDH} + V_{PEPC} + V_{GLYO} - V_{MAL} - V_{NEO} - V_{ASP}) - V_{ACE}$ (17)

3.6. The contribution of the reaction catalysed by the malic enzyme to the formation or degradation of pyruvate gave one more equations.

$V_{MAL} = Ma.V_{PDH}$
$0 = Ma.(V_{KDH} + V_{PEPC} + V_{GLYO} - V_{NEO} - V_{ASP} - V_{ACE}) - (Ma+1).V_{MAL}$ (18)

3.7. The input of carbon entering the cycle via the phosphoenolpyruvate carboxylase catalysed reaction was expressed relatively to that of the citrate synthase catalysed one.

$4 \cdot V_{PEPC} = 2.Pe.(V_{CS})$
$0 = Pe.(V_{KDH} + V_{GLYO} - V_{NEO} - V_{MAL} - V_{ASP}) + (Pe-2).V_{PEPC}$ (19)

So a system of 8 algebraic equations with 8 unknowns (V_{KDH}, V_{PEPC}, V_{GLYO}, V_{MAL}, V_{NEO}, V_{ASP}, V_{ACE}, V_{GLU}) is obtained and allows resolution for the rates as a function of the parameters (Su, Gl, As, Ne, Ac, Ma, Pe) :

$100 = 3.V_{KDH} + 7.V_{PEPC} + 7.V_{GLYO} - 6.V_{MAL} - 3.V_{NEO} - 3.V_{ASP} - V_{ACE}$ (1')
$0 = Su.(3.V_{KDH} + 7.V_{PEPC} - 6.V_{MAL} - 3.V_{NEO} - 3.V_{ASP} - V_{ACE}) + (7.Su-4).V_{GLYO}$ (2')
$0 = As.(5.V_{PEPC} + 5.V_{GLYO} - 5.V_{MAL} - 2.V_{NEO}) - (As+4).V_{ASP}$ (4')
$0 = Ne.(5.V_{PEPC} + 5.V_{GLYO} - 5.V_{MAL} - V_{ASP}) - (2.Ne+3).V_{NEO}$ (5')
$0 = Ac.(V_{KDH} + V_{PEPC} + V_{GLYO} - V_{MAL} - V_{NEO} - V_{ASP}) - V_{ACE}$ (6')
$0 = Ma.(V_{KDH} + V_{PEPC} + V_{GLYO} - V_{NEO} - V_{ASP} - V_{ACE}) - (Ma+1).V_{MAL}$ (7')
$0 = Pe.(V_{KDH} + V_{GLYO} - V_{NEO} - V_{MAL} - V_{ASP}) + (Pe-2).V_{PEPC}$ (8')

For the resolution of this system, we have used the Gauss's method which consist in the triangularisation of the matrix S:

$$
\begin{matrix}
V_{KDH} & V_{PEPC} & V_{GLYO} & V_{MAL} & V_{NEO} & V_{ASP} & V_{ACE} & V_{GLU}
\end{matrix}
$$

$$
\begin{pmatrix}
3 & 7 & 7 & -6 & -3 & -3 & -1 & 0 \\
0 & 5.As & 5.As & -5.As & -2.As & -(4+As) & 0 & 0 \\
0 & 5.Ne & 5.Ne & -5.Ne & -(2.Ne+3) & -Ne & 0 & 0 \\
3.Su & 7.Su & (7.Su-4) & -6.Su & -3.Su & -3.Su & -Su & 0 \\
Ac & Ac & Ac & -Ac & -Ac & -Ac & -1 & 0 \\
Ma & Ma & Ma & -(Ma+1) & -Ma & -Ma & -Ma & 0 \\
Pe & Pe-2 & Pe & -Pe & -Pe & -Pe & 0 & 0 \\
0 & 5.Gl & 5.Gl & -5.Gl & -2.Gl & -Gl & 0 & -5
\end{pmatrix}
=
\begin{pmatrix}
100 \\ 0 \\ 0 \\ 0 \\ 0 \\ 0 \\ 0 \\ 0
\end{pmatrix}
$$

A triangular matrix is then obtained :

$$
\begin{matrix}
V_{KDH} & V_{PEPC} & V_{GLYO} & V_{MAL} & V_{NEO} & V_{ASP} & V_{ACE} & V_{GLU}
\end{matrix}
$$

$$
\begin{pmatrix}
3 & 7 & 7 & -6 & -3 & -3 & -1 & 0 \\
\cdot & 5 & 5 & -5 & -2 & -(1+4/As) & 0 & 0 \\
\cdot & \cdot & -4/Su & 0 & 0 & 0 & 0 & 0 \\
\cdot & \cdot & \cdot & -1/Ma & 0 & 0 & 1/Ac-1 & 0 \\
\cdot & \cdot & \cdot & \cdot & -3/Ne & 4/As & 0 & 0 \\
\cdot & \cdot & \cdot & \cdot & \cdot & \alpha 1 & \alpha 2 & 0 \\
\cdot & \cdot & \cdot & \cdot & \cdot & \cdot & -\frac{\alpha 2.\alpha 3}{\alpha 1}+\alpha 4 & 0 \\
\cdot & \cdot & \cdot & \cdot & \cdot & \cdot & \cdot & -5/Gl
\end{pmatrix}
=
\begin{pmatrix}
100 \\ 0 \\ -100 \\ 0 \\ 0 \\ -100/3 \\ \frac{100.\alpha 3}{3.\alpha 1} - \frac{50.Su}{Pe} \\ \frac{400}{3.\alpha 1.As} + \frac{4.\alpha 2}{(\alpha 4.\alpha 1 - \alpha 2.\alpha 3).As}(\frac{100.\alpha 3}{3.\alpha 1} - \frac{50.Su}{Pe})
\end{pmatrix}
$$

with

$\alpha 1 = -\frac{4}{15}(1+\frac{4}{As}) - \frac{32.Ne}{45.As}$

$\alpha 2 = (\frac{1}{3} - \frac{1}{Ac}) + \frac{Ma}{3}.(1 - \frac{1}{Ac})$

$\alpha 3 = -\frac{2}{5.Pe}(1+\frac{4}{As}) - \frac{16.Ne}{15.Pe.As}$

$\alpha 4 = \frac{1}{Ac} + \frac{2.Ma}{Pe}.(1 - \frac{1}{Ac})$

which gives the solutions:

$V_{GLU} = -\frac{Gl}{5}\left[\frac{400}{3.\alpha 1.As} + \frac{4.\alpha 2}{(\alpha 4.\alpha 1 - \alpha 2.\alpha 3).As}(\frac{100.\alpha 3}{3.\alpha 1} - \frac{50.Su}{Pe})\right]$

$V_{ACE} = \frac{\alpha 1}{(\alpha 4.\alpha 1 - \alpha 2.\alpha 3)}(\frac{100.\alpha 3}{3.\alpha 1} - \frac{50.Su}{Pe})$

$V_{ASP} = \frac{1}{\alpha 1}(-\alpha 2.V_{ACE} - \frac{100}{3})$

$V_{NEO} = \frac{Ne}{3} - \frac{4}{As}.V_{ASP}$

$V_{MAL} = Ma.(\frac{1}{Ac} - 1).V_{ACE}$

$V_{GLYO} = 25.Su$

$V_{PEPC} = \frac{1}{5}\left[(1+\frac{4}{As})V_{ASP} + 2.V_{NEO} + 5.V_{MAL} - 5.V_{GLYO}\right]$

$V_{KDH} = \frac{1}{3}\left[100 + V_{ACE} + 3.V_{ASP} + 3.V_{NEO} + 6.V_{MAL} - 7.V_{GLYO} - 7.V_{PEPC}\right]$

In some cases (where the terms of the diagonal are nil), the initial system had to be rewritten and directly resolved.

II Steady state equations for isotope inflow and outflow. They define the specific activity of any compound in terms of the specific activities of its precursors and the rate of all connecting steps (Connett and Blumm, 1971). One can write the equations of specific activities at isotopic and metabolic steady state, which can be expressed as the rate of influx minus the rate of efflux of label.

As previously described by Borowitz *et al.* (1977) if $V_{i,K}$ and $V_{o,K}$ represent the input and output rates resp. to the Kth intermediate, $S_K(n)$ and $S_N(m)$ represent the specific activity of the nth carbon atom of compound K and of the mth carbon atom of compound N (intermediate precursor of the nth carbon atom of the Kth compound) resp. then for the nth carbon atom of the Kth compound :

$V_{i,K}.S_N(m) - S_K(n).V_{o,K} = 0$

A system of equations is obtained, one for each carbon atom of each intermediate in the metabolic scheme (Fig. 1). The specific activity of each carbon atom is expressed in terms of the fluxes and specific activities of all other carbon atoms from which it received label, according to the known stereochemistry of each reaction :

O_1	$K_1.F_1 + K_2.H_1 = K_3.O_1$	(1)
O_2	$K_1.F_2 + K_2.H_2 = K_3.O_2$	(2)
O_3	$K_1.F_2 + K_2.H_3 = K_3.O_3$	(3)
O_4	$K_1.F_1 + K_2.RE = K_3.O_4$	(4)
F_1	$K_4.X_1 + K_5.(A_1+O_3) + K_6.(O_1+O_4) = K_1.F_1$	(5)
F_2	$K_4.X_2 + K_5.A_2 + K_7.O_2 + K_6.O_3 = K_1.F_2$	(6)
H_1	$K_8.G_4 = K_8.H_1$	(7)
H_2	$K_8.G_5 = K_8.H_2$	(8)
H_3	$K_8.G_6 = K_8.H_3$	(9)
P_1	$K_9.H_1 + K_{10}.O_1 = K_{11}.P_1$	(10)
P_2	$K_9.H_2 + K_{10}.O_2 = K_{11}.P_2$	(11)
P_3	$K_9.H_3 + K_{10}.O_3 = K_{11}.P_3$	(12)
A_1	$K_{11}.P_2 + K_{12}.A_1_1 = K_{13}.A_1$	(13)
A_2	$K_{11}.P_3 + K_{12}.A_1_2 = K_{13}.A_2$	(14)
RE	$RE = (K_{11}.P_3 + K_{13}.O_1 + K_{14}.O_4)/(K_{11} + K_{13} + K_{14})$	(15)

With :

$K_1 = (V_{KDH} + V_{FUM} + V_{GLYO})$
$K_2 = V_{PEPC}$
$K_3 = (V_{KDH} + V_{PEPC} + V_{GLYO} + V_{FUM})$
$K_4 = V_{GLYO}$
$K_5 = V_{KDH}/2$
$K_6 = V_{FUM}/2$
$K_7 = (V_{KDH} + V_{FUM})/2$
$K_8 = (V_{KDH} + V_{GLYO} + 2.V_{PEPC} - 2.V_{MAL} - V_{NEO} - V_{ACE} - V_{ASP})$
$K_9 = (V_{KDH} + V_{GLYO} + V_{PEPC} - 2.V_{MAL} - V_{NEO} - V_{ACE} - V_{ASP})$
$K_{10} = V_{MAL}$
$K_{11} = (V_{KDH} + V_{GLYO} + V_{PEPC} - V_{MAL} - V_{NEO} - V_{ASP} - V_{ACE})$
$K_{12} = V_{ACE}$
$K_{13} = (V_{KDH} + V_{GLYO} + V_{PEPC} - V_{MAL} - V_{NEO} - V_{ASP})$
$K_{14} = (V_{KDH} + V_{NEO} + V_{MAL})$

Since the whole system is interconnected, the specific activity of each carbon of any compound can be written in terms of the specific activities of reference compounds and the various flux rates : we chose the compounds involved in input of carbon into the cycle as the most convenient ones. Namely, we chose as reference carbon atoms the carbons of phosphoenol/pyruvate (H_1, H_2 and H_3), the carbons of fatty acids acetyl units (A_1) and of glyoxysomal derived succinate (X_1 and X_2).

We need the calculation of the individual carbons O_1, O_2, O_3, O_4, A_1, A_2, F_1, F_2, P_1, P_2, P_3 and RE to determine the specific activities of aspartate, glutamate, citrate, malate, alanine and carbons 1 and 5 of glutamate, according to the metabolic scheme (Fig. 1). The resolution of this system was obtained by the Gauss's method, as for the rate system previously resolved.

A matrix was obtained :

	O1	O2	O3	O4	A1	A2	P1	P2	P3	RE	F1	F2		
	K3	·	·	·	·	·	·	·	·	·	-K1	·		K2.G4
	·	K3	·	·	·	·	·	·	·	·	·	-K1		K2.G5
	·	·	K3	·	·	·	·	·	·	·	·	-K1		K2.G6
	·	·	·	K3	·	·	·	·	·	-K2	-K1	·		0
	K6	·	K5	K6	K5	·	·	·	·	·	-K1	·		K4.X1
	·	K7	K6	·	·	K5	·	·	·	·	·	K1	=	K4.X2
	K10	·	·	·	·	·	-K11	·	·	·	·	·		K9.G4
	·	K10	·	·	·	·	·	-K11	·	·	·	·		K9.G5
	·	·	K10	·	·	·	·	·	K11	·	·	·		K9.G6
	·	·	·	K13	·	·	·	K11	·	·	·	·		K12.A11
	·	·	·	·	K13	·	·	·	K11	·	·	·		K12.A12
	a	·	·	b	·	·	·	·	c	-1	·	·		0

with :

$\begin{cases} a = K13/(K11 + K13 + K14) \\ b = K14/(K11 + K13 + K14) \\ c = K11/(K11 + K13 + K14) \end{cases}$

which gave, after triangularisation, the matrix :

O1	O2	O3	O4	A1	A2	P1	P2	P3	RE	F1	F2		
K3	·	·	·	·	·	·	·	·	·	K1	·		
·	K3	·	·	·	·	·	·	·	·	·	K1		
·	·	K3	·	·	·	·	·	·	·	·	K1		
·	·	·	K3	·	·	·	·	·	-K2	·	-K1		
·	·	·	·	K5	·	·	·	·	K2.K6/K3	K1 + 2.K1.K6/K3	K1.K5/K3		
·	·	·	·	·	K5	·	·	·	·	·	K1 + $\frac{K1}{K3}$(K7 - K6)		
·	·	·	·	·	·	-K11	·	·	·	K1.K10/K3	·		
·	·	·	·	·	·	·	-K11	·	·	·	K1.K10/K1		
·	·	·	·	·	·	·	·	K11	·	·	K1.K10/K1	=	v
·	·	·	·	·	·	·	·	·	$\frac{K2.K6.K13}{K1.K5}$	$\frac{K1.K13}{K5}(1-2.\frac{K6}{K3})$	$\frac{K1}{K3}(K10 + K13)$		
·	·	·	·	·	·	·	·	·	·	M5	M6		
·	·	·	·	·	·	·	·	·	·	·	M3		

$v = \begin{pmatrix} K2.G4 \\ K2.G5 \\ K2.G6 \\ 0 \\ -K4.X1 - K2.K6.G4/K3 - K2.K5.G6/K3 \\ K4.X2 - K2.K7.G5/K3 - K2.K6.G6/K3 \\ -K9.G4 - K2.K10.G4/K3 \\ -K9.G5 - K2.K10.G5/K3 \\ -K9.G6 - K2.K10.G6/K3 \\ M1 \\ M2 + (K5.(b.K2-K3).M1)/K2.K6.K13 \\ M4 \end{pmatrix}$

with :

$M1 = K12.A11 + \frac{K4.K13}{K5}.X1 + \frac{K2.K6.K13}{K3.K5}.G4 + \frac{K2.K13}{K3}.G6 + (K9 + \frac{K2.K10}{K3}).G5$

$M2 = -(a.\frac{K2}{K3} + c.\frac{K9}{K11} + c.\frac{K2.K10}{K3.K11}).G4$

$M3 = \frac{K1}{K5}.(K13 - \frac{K7.K13}{K3} - \frac{K6.K13}{K3} - \frac{K10.K5}{K3})$

$M4 = K12.A12 + \frac{K4.K13}{K5}.X2 + \frac{K2.K7.K13}{K3.K5}.G5 + (\frac{K2.K6.K13}{K3.K5} + K9 + \frac{K2.K10}{K3}).G6$

$M5 = \frac{K1}{K3}[a + b + c.\frac{K10}{K11} + \frac{(K3 - 2.K6).(b.K2 - K3)}{K2.K6}]$

$M6 = \frac{K1.K5}{K2.K6.K3.K13}(K10 + K13).(b.K2 - K3)$

whose solutions are :

$F1 = \frac{1}{M5}.(M2 - \frac{K5.(b.K2 - K3)}{K2.K6.K13}.M1 - M6.F2)$

$F2 = \frac{M4}{M3}$

$RE = \frac{K1.K5}{K2.K6.K13}.(\frac{K1.K13}{K5}.(1 - 2.\frac{K6}{K3}).F1 - \frac{K1}{K3}.(K10 + K13).F2 - M1)$

$P1 = \frac{1}{K11}.(\frac{K1.K10}{K3}.F2 + K9.G4 + \frac{K2.K10}{K3}.G4)$

$P2 = \frac{1}{K11}.(\frac{K1.K10}{K3}.F2 + K9.G5 + \frac{K2.K10}{K3}.G5)$

$P3 = \frac{1}{K11}.(\frac{K1.K10}{K3}.F2 + K9.G6 + \frac{K2.K10}{K3}.G6)$

$A1 = \frac{1}{K5}.(-K4.X1 - \frac{K2.K6}{K3}.G4 - \frac{K2.K5}{K3}.G6 - \frac{K1.K5}{K3}.F2 - (\frac{2.K1.K6}{K3} - K1).F1 - \frac{K2.K6}{K3}.RE)$

$A2 = \frac{1}{K5}.(-K4.X2 - \frac{K2.K7}{K3}.G5 - \frac{K2.K6}{K3}.G6 - (\frac{K1.K6}{K3} + \frac{K1.K7}{K3} - K1).F2)$

$O1 = \frac{1}{K3}.(K2.G4 + K1.F1)$

$O2 = \frac{1}{K3}.(K2.G5 + K1.F2)$

$O3 = \frac{1}{K3}.(K2.G6 + K1.F2)$

$O4 = \frac{1}{K3}.(K2.RE + K1.F1)$

In some cases (where the terms of the diagonal are nil), the initial system had, as for the rate system, to be rewritten and directly resolved.